

Non-equilibrium tuning of the thermal Casimir effect

David S. Dean,¹ Bing-Sui Lu,² A. C. Maggs,³ and Rudolf Podgornik²

¹*Univ. Bordeaux and CNRS, Laboratoire Ondes et Matière d'Aquitaine (LOMA), UMR 5798, F-33400 Talence, France*

²*Department of Theoretical Physics, J. Stefan Institute and Department of Physics,*

Faculty of Mathematics and Physics, University of Ljubljana, SI-1000 Ljubljana, Slovenia

³*UMR Gulliver 7083 CNRS, ESPCI ParisTech, PSL Research University, 10 rue Vauquelin, 75005 Paris, France*

In net-neutral systems correlations between charge fluctuations generate strong attractive thermal Casimir forces and engineering these forces to optimize nano-device performance is an important challenge. We show how the normal and lateral thermal Casimir forces between two plates containing Brownian charges can be modulated by decorrelating the system through the application of an electric field, which generates a non-equilibrium steady-state with a constant current in one or both plates, reducing the ensuing fluctuation-generated normal force while at the same time generating a lateral drag force. This hypothesis is confirmed by detailed numerical simulations as well as an analytical approach based on stochastic density functional theory.

PACS numbers: 05.40.-a, 05.20.-y, 05.70.Ln

Electromagnetic (EM) fluctuation-induced interactions are dominant in micro-electro-mechanical systems (MEMS) [1], and their presence is often viewed as undesirable as they engender stiction between the micron-sized components of the MEMS devices. Controlling, or engineering, these forces is, however, difficult as although they are all of electromagnetic origin, they have contributions from both thermal and quantum fluctuations as well as from different microscopic charge multipoles, e.g. ubiquitous dipoles [2] and sometimes also free monopoles [3].

Lifshitz [4] reformulated and generalized the original zero-point electromagnetic field theory of idealized conducting plates, proposed by Casimir [2, 5–7], in terms of the dielectric and magnetic permeabilities of real materials sampled at all Matsubara frequencies including a thermal zero frequency contribution. The Lifshitz formula for EM field fluctuation-induced forces in symmetric interaction configurations between standard materials reveals this interaction is generically attractive [8]. Since the interaction depends on frequency dependent material response properties, it also suggests an immediate means of modulating or even designing the Casimir force by appropriate changes in the material's properties. While this line of reasoning has been followed successfully in meta-materials, it may be more useful to have a means of switching EM fluctuation induced interactions directly *in-situ*. A switch-like induced change in the optical properties of a material indeed yields experimentally measurable differences in the interaction between bodies in a number of cases: e.g. light or laser sources can modify the charge carrier densities in semi-conductors [9, 10], or induce phase changes [11]. Theoretically it has been shown that the quantum Hall effect modified conductivity can also be used to modify Casimir forces between graphene sheets [12]. Holding interacting materials at different temperatures also allows modifications of Casimir interactions [13–21].

An alternative to the Lifshitz field-based formulation is

presented by the Schwinger matter-based approach where the Casimir force originates in interactions between fluctuating charges and currents [6, 22, 23]. Within this conceptual framework the attraction between materials can be understood as being due to correlations between microscopic EM source charge fluctuations that in general reduce their (free) energy. This implies that the effect of non-equilibrium driving the sources with an external electric/magnetic field will *scramble* the system's ability to develop charge correlations and could thus in general reduce the attraction between the materials. The scenario of engineering the EM fluctuation interactions by applying external driving fields to MEMS is relatively easily implemented, compared to the switching mechanisms based on material properties modifications discussed above, and thus may be a promising technological direction worth pursuing in detail.

In order to test the non-equilibrium driving hypothesis and assess its ramifications, we analyze the system of two parallel conducting plates, where only one of them is subjected to a current-inducing applied external electric field in a closed circuit configuration. For systems with currents the usual methods of equilibrium statistical mechanics do not apply. We propose a methodology to study the effect of an imposed current in the non-equilibrium steady state configuration on both the normal and lateral forces. The response of these forces to driving is surprisingly rich and this study thus opens up new perspectives for direct *in situ* control of the EM fluctuation interactions.

We analyze a well defined classical 2D jellium model, which can be studied out-of-equilibrium both numerically and analytically, composed of two parallel plates with mobile charged Brownian particles embedded within a uniform background charge sheet [24–26], see Fig. (1). In equilibrium, at high temperatures in the weak coupling limit, the two plates exhibit the universal thermal Casimir force $F_{\perp} = -\frac{T\zeta(3)}{8\pi L^3}$ at large inter-plate separa-

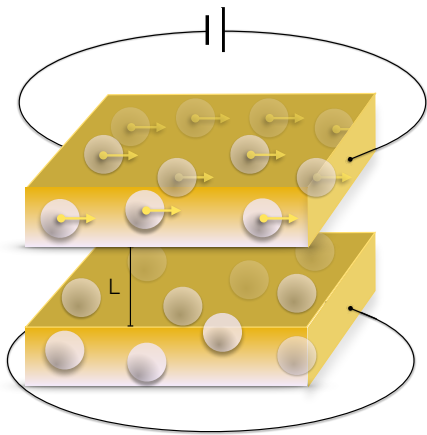


FIG. 1. (color online) Schematic depiction of plates (1 and 2) containing mobile charges, with an external electric field \mathbf{E}_{01} applied to plate 1 in a closed circuit configuration, driving a current flow in the plate set up using a battery. The circuit of both plates [27] is open so charge flows through the system rather than accumulating at the edges of the plates.

tions L , with S denoting the area of the plates, ζ is the Riemann zeta function, and T is the temperature of the two plates, assumed to be the same for both. To explore the effect of an electric field on one of the plates we need to specify the dynamics of the charges and we adopt a Langevin model [21, 33] where a charge in the plate α at the point \mathbf{X} obeys the over-damped Langevin equation

$$\frac{d\mathbf{X}}{dt} = \beta D_\alpha q_\alpha \mathbf{E}_{||\alpha}(\mathbf{X}) + \sqrt{2D_\alpha} \boldsymbol{\eta}_\alpha, \quad (1)$$

where $\boldsymbol{\eta}_\alpha$ is a zero-mean Gaussian white noise with correlation function $\langle \eta_{\alpha i}(t) \eta_{\alpha' j}(t') \rangle = \delta_{\alpha\alpha'} \delta_{ij} \delta(t-t')$ and $\mathbf{E}_{||\alpha}(\mathbf{X})$ is the local in plane electric field in the plate α , generated by the electric charge distributions in both plates as well as any externally applied electric field. In addition, D_α denotes the diffusion constant of the charges and β [28] the inverse temperature so that βD_α is the local mobility, as deduced from the Einstein relation. Finally, q_α is the charge of the mobile Brownian particles in the plate α and if \bar{n}_α denotes the average density of charge carriers in plate α ; the the uniform neutralising surface charge density is thus $\sigma_\alpha = -\bar{n}_\alpha q_\alpha$. The idealized model above is amenable to both detailed numerical as well as analytical developments, confirming our basic hypothesis that the driving field modifies the charge correlation between the plates, thus leading to a modified thermal Casimir force in direction normal as well as lateral to the plates.

Numerical simulations: The two-plate system was simulated by integrating the Langevin equations Eq. (1) for Brownian particles [30]; the electrostatic forces due to the charges are computed via Ewald summation. We use a non-cubic box of dimensions $H \times H \times 3H$. with peri-

odic boundary conditions in each direction. We studied several separations between the plates up to a maximum distance of $L = 0.12H$; beyond this distance the interaction between plates can be shown to cross-over to an exponential form due to the discrete Fourier modes within the simulation box. In this non-cubic geometry the undesired interactions between images of plates in the z -direction are known to be negligible [29]. We worked with a variable total number of particles, $N = 1000$, $N = 2000$, $N = 4000$ in order to control finite size errors in the simulation. Apart from the applied electric field \mathbf{E}_{01} , causing a current to flow within plate 1, the two plates are identical (the charges are identical and of the same number $N/2$ in each plate, the diffusion constants and temperatures are also the same). Plate separations are taken such that we find the far field universal Casimir effect at zero applied field.

The normal and lateral force acting on the plate α are computed from the formulas

$$\mathbf{F}_{\perp,||\alpha}(L) = q_\alpha \int_{S_\alpha} d^2\mathbf{x} \mathbf{E}_{\perp,||\alpha}(\mathbf{x}) \Delta n_\alpha(\mathbf{x}), \quad (2)$$

where $n_\alpha(\mathbf{x}) = \sum_i \delta(\mathbf{X}_i - \mathbf{x})$ is the density of mobile charge carriers and $\Delta n_\alpha(\mathbf{x}) = n_\alpha(\mathbf{x}) - \bar{n}_\alpha$ is the fluctuation about its spatially averaged value \bar{n}_α , which is the same as that of the neutralizing uniform background charge. In Eq. (2) $\perp, ||$ indicates the direction with respect to the bounding plates. The electrostatic potential $\phi(\mathbf{x})$ in the plate α has contributions both from the plate α as well as plate α' (opposite) mediated by the standard Coulomb interaction, while the dielectric constant ϵ is assumed to be homogeneous.

The numerical results for the average of the two forces are plotted in Fig. 2. They are both fluctuational in nature, and in principle the statistics of the force can be measured. For small driving fields the normal Casimir force saturates to the equilibrium thermal Casimir force, while the lateral force vanishes in equilibrium. As the field increases there is a *monotonic* decrease in the amplitude of the normal force, that eventually asymptotes to zero, and a *non-monotonic* variation of the lateral force that is zero for small as well as large values of the driving field.

Dynamical density functional theory The density fields $n_\alpha(\mathbf{x}, t)$ in each plate evolve according to the exact stochastic partial differential equation [31, 32]

$$\begin{aligned} \frac{\partial n_\alpha(\mathbf{x}, t)}{\partial t} &= D_\alpha \nabla_{||} \cdot [\nabla_{||} n_\alpha(\mathbf{x}, t) - \beta_\alpha q_\alpha \mathbf{E}_{||\alpha} n_\alpha(\mathbf{x}, t)] \\ &+ \nabla_{||} \cdot [\sqrt{2D_\alpha n_\alpha(\mathbf{x}, t)} \boldsymbol{\eta}_\alpha(\mathbf{x}, t)]. \end{aligned} \quad (3)$$

In this density representation of the dynamics, the noise $\boldsymbol{\eta}_\alpha(\mathbf{x}, t)$ is a spatio-temporal Gaussian white noise vector field of mean zero and with correlation function $\langle \eta_{\alpha i}(\mathbf{x}, t) \eta_{\alpha' j}(\mathbf{x}', t') \rangle = \delta_{\alpha\alpha'} \delta_{ij} \delta(t-t') \delta(\mathbf{x} - \mathbf{x}')$.

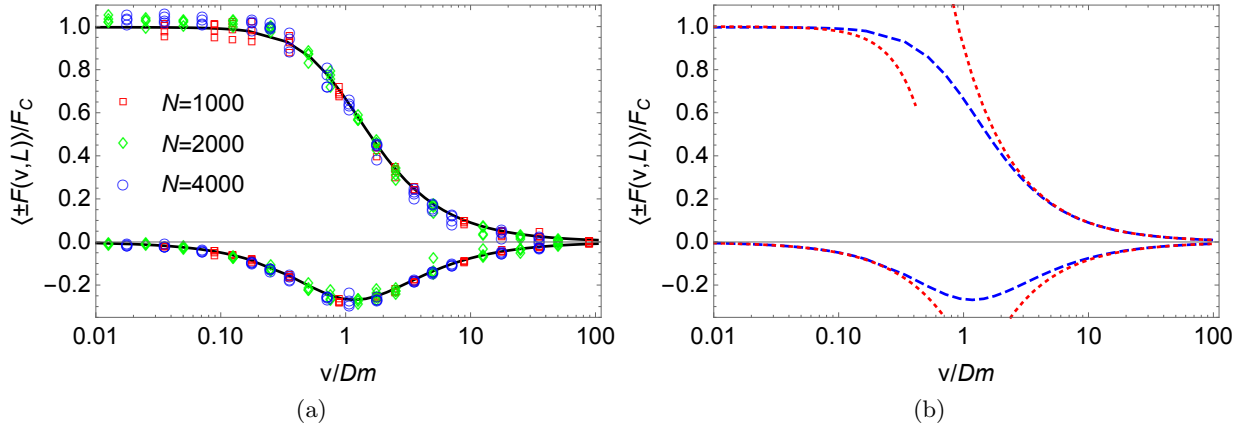


FIG. 2. (color online) (a): Evolution of the amplitude of the perpendicular and transverse components of the Casimir force with the driving field, normalized by the thermal Casimir force, $F_C = -TS\zeta(3)/8\pi L^3$. For ease of comparison, we have displayed the component of the normalized tangential force that is parallel to the driving field, with a sign opposite to that of the normalized perpendicular force. Simulation results are taken from systems with $N = 1000$ (red squares), $N = 2000$ (green diamonds) and $N = 4000$ (blue circles). For each value of N the interaction is evaluated for four separations: $L = 0.02H$, $L = 0.05H$, $L = 0.08H$, $L = 0.12H$. The vertical data spread correspond to residual systematic, finite size errors in the simulations. The theoretical predictions, Eqs. (9, 10), for $L \times m = 2000$ are shown by black solid curves. (b): Evolution of the amplitude of the perpendicular and transverse components of the Casimir force between identical plates ($D_1 = D_2 = D$, $m_1 = m_2 = m$) with the driving field, normalized by the universal thermal Casimir force. Theoretical predictions, Eqs. (9, 10), for $Lm = 2000$ are shown by blue dashed curves, whilst the corresponding small field and large field asymptotes, Eqs. (11, 12, 13, 14), are shown as the red, dotted curves.

To make analytical progress we expand the deterministic term in Eq. (3) to linear order in the density fluctuations n_α and the noise term to zeroth order (since it is of zero mean this is consistent with the first order expansion of the deterministic terms). This approximation has already been used to examine interactions between plates out of equilibrium in e.g. evolution to the equilibrium force for initially out of equilibrium plates [33], as well as for the non-equilibrium force between plates held at different temperatures [21]. This small density expansion was recently shown to reproduce Onsager's classical results on the conductivity of strong electrolyte solutions [38] in a very straightforward and compact manner [35]. Within the small density fluctuation approximation the two dimensional Fourier transform of the density fluctuations, defined as $\Delta \tilde{n}_\alpha(\mathbf{Q}, t) = \int_{S_\alpha} d^2\mathbf{x} \exp(-i\mathbf{Q} \cdot \mathbf{x}) \Delta n_\alpha(\mathbf{x}, t)$, has a steady state correlation function $\langle \Delta \tilde{n}_\alpha(\mathbf{Q}) \Delta \tilde{n}_{\alpha'}(\mathbf{Q}') \rangle = (2\pi)^2 \delta(\mathbf{Q} + \mathbf{Q}') C_{\alpha\alpha'}(\mathbf{Q})$ which obeys

$$M_{\alpha\gamma}(\mathbf{Q}) C_{\gamma\alpha'}(\mathbf{Q}) + C_{\alpha\gamma}(\mathbf{Q}) M_{\gamma\alpha'}^\top(-\mathbf{Q}) = 2\delta_{\alpha\alpha'} D_\alpha \bar{n}_\alpha Q^2. \quad (4)$$

The matrix $M(\mathbf{Q})$ is given by

$$M_{\alpha\gamma}(\mathbf{Q}) = Q^2 \left(\tilde{D}_\alpha \delta_{\alpha\gamma} + \beta q_\alpha q_\gamma \bar{n}_\gamma D_\alpha \tilde{G}(\mathbf{Q}, z_{\alpha\gamma}) \right), \quad (5)$$

where $\tilde{D}_\alpha = D_\alpha (1 - i\beta q_\alpha \bar{n}_\alpha \hat{\mathbf{Q}} \cdot \mathbf{E}_{0\alpha} / Q)$, $z_{\alpha\gamma} = z_\alpha - z_\gamma$ and $\hat{\mathbf{Q}}$ is the unit wave-vector. The term $\tilde{G}(\mathbf{Q}, z_{\alpha\gamma})$ denotes the in-plane Fourier transform of the Coulomb

interaction $G(\mathbf{x}, z)$ (without the charge factors) and is given by $\tilde{G}(\mathbf{Q}, z) = \exp(-Q|z|)/2\epsilon Q$. The components of the fluctuation force in Eq. (2) can be expressed as

$$\langle F_\perp \rangle = -q_1 q_2 \int_{S_1} d\mathbf{x} \int_{S_2} d\mathbf{y} \langle \Delta n_1(\mathbf{x}) \Delta n_2(\mathbf{y}) \rangle \frac{\partial G(\mathbf{x} - \mathbf{y}, L)}{\partial L} \quad (6)$$

and

$$\langle \mathbf{F}_\parallel \rangle = -q_1 q_2 \int_{S_1} d\mathbf{x} \int_{S_2} d\mathbf{y} \langle \Delta n_1(\mathbf{x}) \Delta n_2(\mathbf{y}) \rangle \nabla_\parallel G(\mathbf{x} - \mathbf{y}, L). \quad (7)$$

The Fourier transform of $\langle \Delta n_\alpha(\mathbf{x}) \Delta n_\beta(\mathbf{y}) \rangle$ can then be obtained from Eq. (4), which together with the definitions Eqs. (6), (7) yield the average normal and lateral force. Defining

$$f(Q, L) = \log \left(1 + \Delta(\mathbf{v}_1, \mathbf{v}_2)^2 - \frac{m_1 m_2 \exp(-2QL)}{(m_1 + 2Q)(m_2 + 2Q)} \right) \quad (8)$$

with $\mathbf{v}_\alpha = \beta q_\alpha D_\alpha \mathbf{E}_{0\alpha}$ the average velocity of the mobile charges in the plate α , $m_\alpha = \beta \bar{n}_\alpha q_\alpha^2 / \epsilon$ is the inverse screening length for a 2D Coulomb gas of mobile charges in equilibrium and $\Delta(\mathbf{v}_1, \mathbf{v}_2) = 2(\hat{\mathbf{Q}} \cdot (\mathbf{v}_1 - \mathbf{v}_2)) / (D_1 m_1 + D_2 m_2 + 2(D_1 + D_2)Q)$, we can write [30]

$$\langle F_\perp(L) \rangle = -\frac{1}{2} TS \int \frac{d^2\mathbf{Q}}{(2\pi)^2} \frac{\partial f(Q, L)}{\partial L}, \quad (9)$$

and

$$\langle \mathbf{F}_{\parallel}(L) \rangle = TS \int \frac{d^2 \mathbf{Q}}{(2\pi)^2} \frac{\partial f(Q, L)}{\partial L} \hat{\mathbf{Q}} \Delta(\mathbf{v}_1, \mathbf{v}_2). \quad (10)$$

We note that when $\mathbf{v}_1 - \mathbf{v}_2 = 0$ we recover the expression for the equilibrium thermal Casimir force for $\langle F_{\perp}(L) \rangle$, while the lateral force is zero, since in the common rest frame of the moving charges the system is in equilibrium.

The normal force is monotonic in its variation with respect to the relative difference of the bare velocity of the charges in each plate. In the far field limit where $L \gg m_1^{-1}, m_2^{-1}$ and when in addition $|\mathbf{v}_1 - \mathbf{v}_2| \ll u_1, u_2$, where $u_{\alpha} = D_{\alpha} m_{\alpha}$ define an intrinsic velocity scale in each plate, the average force simplifies to give

$$\langle F_{\perp}(L) \rangle \approx -\frac{TS}{8\pi L^3} \left[\zeta(3) - \frac{\pi^2 |\mathbf{v}_1 - \mathbf{v}_2|^2}{3(u_1 + u_2)^2} \right]. \quad (11)$$

The effect of the applied field can thus be seen as renormalizing the effective *Hamaker* constant associated with the $1/L^3$ power law. The far field fluctuation induced attraction between the plates thus monotonically decreases upon increasing the relative velocity. In the opposite limit of large relative velocity, we find that the force decays as

$$\langle F_{\perp}(L) \rangle \approx -\frac{TS}{32\pi L^3} \frac{(u_1 + u_2)}{|\mathbf{v}_1 - \mathbf{v}_2|} \left[8 - \frac{\pi^2}{3} - 8 \ln 2 + 4 \ln^2 2 \right] \quad (12)$$

Contrary to the normal force, the lateral force is not monotonic in the relative velocity and shows a well defined maximum. On the two sides of this minimum the lateral force behaves as

$$\langle F_{\parallel}(L) \rangle \approx -\frac{TS}{16\pi L^3} \frac{(u_1 + u_2)}{|\mathbf{v}_1 - \mathbf{v}_2|} \quad (13)$$

in the large field limit, and for small fields as

$$\langle F_{\parallel}(L) \rangle \approx -\frac{TS |\mathbf{v}_1 - \mathbf{v}_2|}{8\pi L^3 (u_1 + u_2)} \left[\zeta(3) - \frac{\pi^2 |\mathbf{v}_1 - \mathbf{v}_2|^2}{128(u_1 + u_2)^2} \right]. \quad (14)$$

A similar non-monotonic drag force has recently been predicted for single particles coupled to thermally fluctuating classical fields [36, 37].

In Fig. 2a we compare the theoretical predictions, Eqs. (9, 10), for the normal and lateral forces with the results of our numerical simulations. We see that, despite the relatively low temperature of the system, the agreement for both forces is excellent. The asymptotic results for the small and large field limits, Eqs. (11, 12, 13, 14), are compared to the full numerical integration of Eqs. (9, 10) in Fig. 2b.

Conclusions: We have introduced a simple model exhibiting the thermal Casimir effect and shown that when

the system is driven by an external electric field, the thermal Casimir force, both its normal and lateral components, can be modulated in a controlled and reversible manner. The underlying physical mechanism is that the external driving electric fields suppress the charge correlations which are responsible for the fluctuation interaction. Indeed the Onsager study of the field dependence of electrolyte conductivity [38], the Wien effect, shows that the increase in conductivity is due to the fact that the applied field suppresses Debye screening. The underlying mechanism here is clearly related and we have clearly exhibited the effect in numerical simulations, and analytically, taking into account all the non-equilibrium physics in the model via its microscopic formulation. Indeed one of the prime advantages of the model studied here is that one can carry out numerical experiments to measure fluctuation induced interactions *out of equilibrium* and future study of this model should enable the study of fluctuation induced interactions beyond the weak density fluctuation approximation employed in our analytical study.

Extensions of this model to more realistic systems/models are clearly desirable in order to test the general hypothesis on field induced correlation scrambling put forward here. Another natural question to ask is whether non-equilibrium forcing can be used to amplify correlations and thus enhance the fluctuation induced attractive force? The Brownian conductor model should be extended to take into account inertial effects so that it more closely resembles the Drude model. In addition, retardation effects in the electromagnetic interactions between the charges could also be incorporated. Ultimately one should consider non-equilibrium quantum field theories in order to understand the quantum aspects of the problem. Clearly AC driving fields also constitute an interesting line of research, from both a numerical and analytical point of view.

This work was partially financed by a Joliot Chair of the ESPCI (RP), the ANR FISICS (DSD), the ANR FSCF (ACM), and ARRS P1-0055 (BSL).

-
- [1] P. Ball, *Nature* **447**, 772 (2007).
 - [2] V. Mostepanenko, N. N. Trunov, *The Casimir Effect and Its Applications*, (Oxford Science Publications), Oxford University Press, USA (1997).
 - [3] D. Drosdoff, I.V. Bondarev, A. Widom, R. Podgornik, L.M. Woods, *Phys. Rev. X* **6**, 011004 (2016).
 - [4] E. M. Lifshitz, *Soviet Physics JETP* **2**, 73 (1956).
 - [5] H. B. G. Casimir, *Proc. Koninklijke Nederlandse Akad. Wetenschappen* **B51**, 793 (1948).
 - [6] K A Milton, *The Casimir Effect, Physical Manifestations of Zero-Point Energy*, World Scientific Publishing UK (2001).
 - [7] D. Dalvit, P. Milonni, D. Roberts, F. Rosa, *Casimir Physics*, Lecture Notes in Physics Volume 834, Springer-Verlag Berlin Heidelberg (2011).

- [8] V. A. Parsegian, *Van der Waals Forces*, Cambridge (Cambridge) (2006).
- [9] W. Arnold, S. Hunklinger, and K. Dransfeld, *Phys. Rev. B*, **19**, 6049 (1979).
- [10] F. Chen, G. L. Klimchitskaya, V. M. Mostepanenko, and U. Mohideen *Phys. Rev. B* **76**, 035338 (2007).
- [11] G. Torricelli, P. J. van Zwol, O. Shpak, C. Binns, G. Palasantzas, B.J. Kooi, V. B. Svetovoy, M. Wuttig, *Phys. Rev. A (R)* **82** 010101 (2010).
- [12] W.-K. Tse and A. H. MacDonald, *Phys. Rev. Lett.* **109**, 236806 (2012).
- [13] I.A. Dorofeyev, *J. Phys. A: Math. Gen.* **31**, 4369 (1998).
- [14] M. Antezza, L.P. Pitaevskii and S. Stringari, *Phys. Rev. Lett.* **95**,113202 (2005).
- [15] M. Antezza, L.P. Pitaevskii, S. Stringari and V.B. Svetovoy, *Phys. Rev. A* **77**,022901 (2008).
- [16] G. Bimonte, *Phys. Rev. A.* **80**, 042102 (2009).
- [17] M. Krüger, T. Emig, G. Bimonte and M. Kardar, *Europhys. Lett.* **95**,21002 (2011).
- [18] M. Krüger, T. Emig and M. Kardar, *Phys. Rev. Lett.***106**, 210404 (2011).
- [19] R. Messina and M. Antezza, *Europhys. Lett.* **95**, 61002 (2011).
- [20] A.W. Rodriguez, O. Ilic, P. Bermel, I. Celanovic, J.D. Joannopoulos, M. Soljačić and S.G. Johnson, *Phys. Rev. Lett.* **107** 114302 (2011).
- [21] B.-S. Lu, D.S. Dean, and R. Podgornik, *Europhys. Lett.* **112**, 20001 (2015).
- [22] R.L. Jaffe, *Phys. Rev. D* **72**, 021301(R) (2005).
- [23] J. Cugnon, *Few-Body Syst.* **53**, 181 (2012).
- [24] Y. Levin, *Physica A* **265**, 432 (1999).
- [25] P.R. Buenzli and Ph. A. Martin, *Europhys. Lett.* **72** 42 (2005).
- [26] B. Jancovici and L. Samaj, *Europhys. Lett.* **72**35 (2005).
- [27] If the circuit of plate 2 is closed, a current is induced in the plate 2 by the *Coulomb drag* due to plate 1, this is the case considered here. If the circuit of the opposing plate is open, charge accumulates at the plate edges, creating an in-plane electrical field which cancels the due to the driven plate and prevents current flow in the opposing plate. This open configuration can be studied both numerically and analytically and is left for further study.
- [28] An electric current in one plate will lead to a steady state where this plate will have a higher temperature than the other. A difference in temperature can be taken into account in both our numerical and analytic treatment [21] of the problem, however for the sake of simplicity it is not studied in this letter.
- [29] I.-C. Yeh and M. L. Berkowitz, *J. Chem. Phys.* **111**, 3155 (1999).
- [30] For further details see supplementary material, which includes Refs. [1–4].
- [31] D.S. Dean, *J. Phys. A: Math. Gen.* **29**, 613 0 (1996).
- [32] K. Kawasaki, *Physica A* **208**, 35 (1994).
- [33] D.S. Dean and R. Podgornik, *Phys. Rev. E* **89**, 032117 (2014).
- [34] R. Zwanzig, *Non equilibrium statistical mechanics*, Oxford University Press, Oxford (2001).
- [35] V. Démery and D.S. Dean, *J. Stat. Mech.* **2016**, 023106 (2016).
- [36] V. Démery and D.S. Dean, *Phys. Rev. Lett.* **104**, 080601 (2010).
- [37] V. Démery and D.S. Dean, *Phys. Rev. E* **84**, 010103(R) (2011).
- [38] P.C. Hemmer, H. Holden and S. Kjelstrup Ratkje eds. *The collected works of Lars Onsager (with commentary)*, World Scientific (Singapore) (1996).
- [39] H. Flyvbjerg and H. G. Petersen, *J. Chem. Phys.* **91**, 461(1989).
- [40] A. S. Kronfeld, *Progress of Theoretical Physics Supplement*, **111**, 293 (1993).
- [41] E. Wigner *Phys. Rev.* **40**, 749, (1932).
- [42] J.J. Weis, D. Levesque, and J.M. Caillol, *J. Chem. Phys.*, **109**, 7486, (1998).

SUPPLEMENTARY MATERIAL

Numerical simulations

We used the standard three-dimensional formulation of the Ewald summation introducing a real-space range α . The complementary long-range part of the interaction is calculated in Fourier space, requiring modes out to wave-vectors $q_m \sim 1/\alpha$. The interaction energy as well as the forces are independent of α which can then be used to optimize the speed of the calculation. Balancing the effort in real and Fourier space leads to a value of α which decreases with the number of simulated particles so that the computer effort to calculate the force on all of the particles scales as $O(N^{8/5})$, with N the number of particles. In practice, for each value of N , we made a series of test runs with variable α chosen to produce the most rapid code. We used a relative precision of 10^{-11} in the Ewald evaluation.

We integrated the Langevin equation using the Euler method with a time step dt . We chose this step as follows: First we performed a series of short simulations with very large time steps to find the stability limit of the integrator. We then divided this value of dt by 100 to find a stable regime where integration errors are not too large. We performed high statistics simulations for different time steps about our first estimate for the production time step. We measured the force between plates with statistical errors better than 2%, estimated using the method of [1], and found the value of dt which also gives systematic errors of order of 2%. In practice it is immediately clear when the step size has been chosen too large when comparing several different simulations.

We note that the effect of a finite step size can be studied analytically using the concept of *inverse error analysis*. A set of variables i with energy function \mathcal{H} when simulated by a Euler integrator generates an equilibrium measure characterised by an effective energy [2]

$$\bar{\mathcal{H}} = \mathcal{H} + \frac{Ddt}{4} \sum_i (2\nabla_i^2 \mathcal{H} - \beta(\nabla_i \mathcal{H})^2), \quad (15)$$

where D is the particle diffusion constant. When applied to a pair of Coulomb particles this gives an extra effective potential in dt/r^4 . Remarkably this correction

is very similar to the Wigner expansion [3] in quantum mechanics. The integration error looks very much like the quantum Casimir interaction in the high temperature limit, with dt playing a role comparable to \hbar^2 .

With the choice of the time step set as above, we performed preliminary simulations in order to choose the temperature and the number of particles for the main simulations. In these initial studies we found that finite size corrections are rather strong, requiring a large number of particles to observe the correct asymptotic form of the Casimir interaction at zero driving field. We interpret this as a consequence of the unusual form of screening in quasi-two-dimensional plasmas, coupled through the three dimensional Coulomb interaction, which leads to a charge structure factor, in the Debye-Hückel limit (for a single plate), of the form [4]

$$S(\mathbf{Q}) = \frac{|\mathbf{Q}|}{(|\mathbf{Q}| + m/2)} \quad (16)$$

with $m = q^2 \bar{n} \beta / \epsilon$ and $\bar{n} = N/H^2$. This singular form in $|\mathbf{Q}|$ leads to a power-law decay of correlations in real space [4], in contrast to the exponential decay of correlations in three-dimensional plasmas. We chose to run our simulations at a temperature such the Bjerrum length is comparable to the particle separation; specifically we took the values $T = 1.03 q^2 \sqrt{\bar{n}} / (4\pi\epsilon)$. This corresponds to a region intermediate between the high and low temperature limits. Simulations at lower temperatures showed strong deviations from the Debye-Hückel structure factor, in particular $S(\mathbf{Q})$ develops a weak peak. At large temperatures the screening length m^{-1} becomes large, physically thermal fluctuations destroy screening, and the far field limit is pushed to distances L comparable to the system size and thus into a region where finite size corrections become very important.

We finally chose a series of systems with three different values of N : $N = 1000, 2000, 4000$. With these numbers of particles the un-driven systems shows a Casimir interaction, with the correct amplitude, over a range of separations from $0.02H$ to $0.12H$. A simulation for $N = 500$

showed strong modification of the Casimir amplitude for the separation of $0.02H$. Proper scaling of the data as the number of particles increases is a strong test of being in the continuum limit.

For the values of N that we study and separations below $0.02H$ we cross-over into a single particle regime, rather than a collective Casimir regime. For separations large than $0.12H$ there is an exponential decay of interactions, coming from the discrete nature of Fourier modes within a box. Within this range of distances Fig. (2) in the main text shows that we control systematic errors at zero driving force to within about 2%. The largest systems that we study require one month of simulation per point, to reduce statistical errors to within 2%. The residual vertical spread in the points of Fig. (2) is dominated by finite size corrections, which would require larger numbers of particles to reduce further.

With a series of systems calibrated at zero driving force we performed the final series of simulations to measure interactions as a function of driving field. We note that at the largest driving field it is necessary to re-calibrate the criterion for the choice of dt : Relative motion of driven/un-driven particles is the fastest process in the simulation, which must be well resolved to generate accurate results. The data presented is evaluated for an electric field which is skewed compared to the simulation cell. Other simulations (data not shown) show that the curves of Fig. 2 become anisotropic for the largest fields that we studied. This anisotropy can be understood by the fact that the driving reduces the effective number of interacting modes contributing to the Casimir interactions. This small number of modes in the summation then leads to angular modulation of the curves. This anisotropy can be treated analytically within the stochastic density functional theory by replacing the Fourier integrals in Eqs. (9, 10) by a discrete Fourier sum.

Analytical results for the force

The compact form of Eqs. (9, 10), as derived from Eq. (8), are deduced from the expressions

$$\langle F_{\perp}(L) \rangle = -TS \int \frac{d^2\mathbf{Q}}{(2\pi)^2} \frac{Q m_1 m_2 \exp(-2QL)}{(m_1 + 2Q)(m_2 + 2Q) \left(1 + \frac{4(\mathbf{Q} \cdot (\mathbf{v}_1 - \mathbf{v}_2))^2}{Q^2(D_1 m_1 + D_2 m_2 + 2(D_1 + D_2)Q)^2} \right) - m_1 m_2 \exp(-2QL)}, \quad (17)$$

$$\begin{aligned} \langle \mathbf{F}_{\parallel}(L) \rangle = & -TS \int \frac{d^2\mathbf{Q}}{(2\pi)^2} \frac{2m_1 m_2 e^{-2QL}}{(m_1 + 2Q)(m_2 + 2Q) \left(1 + \frac{4(\mathbf{Q} \cdot (\mathbf{v}_1 - \mathbf{v}_2))^2}{Q^2(D_1 m_1 + D_2 m_2 + 2(D_1 + D_2)Q)^2} \right) - m_1 m_2 e^{-2QL}} \\ & \times \frac{(\mathbf{Q} \cdot (\mathbf{v}_1 - \mathbf{v}_2))\mathbf{Q}}{Q(D_1 m_1 + D_2 m_2 + 2(D_1 + D_2)Q)}, \end{aligned} \quad (18)$$

which are derived from Eqs. (6) and (7) under averaging and using the density fluctuation correlation functions

derived from Eq. (4).

-
- [1] H. Flyvbjerg and H. G. Petersen, J. Chem. Phys. **91**, 461(1989)
- [2] A. S. Kronfeld Progress of Theoretical Physics Supplement (1993) **111**, 293-311.
- [3] E. Wigner Phys. Rev. **40**, 749, (1932).
- [4] J.J. Weis, D. Levesque, and J.M. Caillol, J. Chem. Phys., **109**, 7486-7497, (1998).